Patient stratification reveals the molecular basis of disease comorbidities

Beatriz Urda-García[1,2], Jon Sánchez-Valle[1,*], Rosalba Lepore[1,3] and Alfonso Valencia[1,4,*]

[1]Barcelona Supercomputing Center (BSC), Barcelona, 08034

[2]Department of Experimental and Health Sciences, Universitat Pompeu Fabra, Barcelona, Spain

[3]Department of Biomedicine, Basel University Hospital and University of Basel, Basel, Switzerland

[4]ICREA, Barcelona, 08010 Spain.

*Correspondence to: jon.sanchez@bsc.es and alfonso.valencia@bsc.es

Abstract

Epidemiological evidence shows that some diseases tend to co-occur; more exactly, certain groups of patients with a given disease are at a higher risk of developing a specific secondary condition. Despite the considerable interest, only a small number of connections between comorbidities and molecular processes have been identified.

Here we develop a new approach to generate a disease network that uses the accumulating RNA-seq data on human diseases to significantly match a large number of known comorbidities, providing plausible biological models for such co-occurrences. Furthermore, 64% of the known disease pairs can be explained by analysing groups of patients with similar expression profiles, highlighting the importance of patient stratification in the study of comorbidities.

These results solidly support the existence of molecular mechanisms behind many of the known comorbidities. All the information can be explored on a large scale and in detail at http://disease-perception.bsc.es/rgenexcom/.

Introduction

Disease comorbidity is defined as the co-occurrence of two or more conditions in the same patient[1]. Comorbidity incidence increases with age and has a high impact on life expectancy, as it increases patient mortality and complicates the choice of therapies, posing a major problem for patients and health care systems. Accumulating evidence from epidemiological studies indicates that such co-occurrences do not appear randomly and that specific trends are observed, with some diseases co-occurring more than expected by chance[2,3]. Systematic studies using electronic health records have been performed to analyze comorbidity patterns in a given population where disease co-occurrences are represented by static networks[2,3] or network trajectories if their progression over time is considered[4]. These studies demonstrated the predictive value of comorbidity patterns to determine disease progression and outcome, including mortality risk.

The observed patterns suggest that comorbid diseases might share underlying molecular mechanisms and risk factors, which can be both genetic and environmental, such as drug exposure and lifestyle. Thus, a better understanding of the molecular mechanisms behind comorbidities is a crucial step towards improved prevention, diagnosis, and treatment of these conditions.

Recent studies on disease comorbidities have included molecular information often analyzing pairs of diseases based on shared disease-related genes[5]. Similar to functionally related genes, disease-associated genes tend to colocalize in the protein-protein interaction network forming disease modules which can aid the identification of novel candidate genes and inform about disease associations, including phenotypic similarity and comorbidities[6]. In this context, previous work showed that the overlapping gene expression signatures between several Central Nervous System disorders (CNSd) and cancer types could inform about the molecular mechanisms underlying their direct and inverse comorbidities[7,8]. More recently, we have observed that disease similarity networks based on gene expression profiles can be used to identify known comorbidity relationships[8]. Although these efforts were able to capture interesting examples, they were unable to recapitulate what is known at the medical level in a systematic manner. The mentioned approaches based on PPIs and microarrays reproduced a very small percentage of the epidemiology, and other networks based on miRNAs[9] and the microbiome[10] had no capacity for it. Hence, we address the still largely unknown extent to which molecular information can provide a general explanation to disease comorbidities.

Here, we reformulate the problem and we show, for the first time, that gene expression data is definitively able to reproduce medically known disease co-occurrences. To achieve that, we integrate

56 publicly available RNA-seq data sets, which are currently replacing microarrays due to their improved
57 sensitivity, reproducibility, and detection's dynamic range[11,12]. We characterize the gene expression
58 signature of human diseases based on differential expression and functional enrichment analyses. Then,
59 we generate a disease similarity network based on the similarities between diseases' differential
60 expression profiles. Afterwards, we build a stratified similarity network grouping patients of the same
61 disease with a similar expression profile (here called meta-patients), addressing the fact that patients
62 suffering from a given disease present different risks of developing specific secondary conditions, as
63 evidenced by the Danish medical records[4]. Both networks are able to significantly recapitulate a large
64 proportion (up to 64%) of the medically known comorbidities[2], providing a well-defined set of pathways
65 and molecular functions potentially implicated in disease comorbidities, which can be analyzed at
66 http://disease-perception.bsc.es/rgenexcom/.

67

68 # Results

69 **Gene expression fingerprint of human diseases**

70 First, we collected published studies analyzing human diseases with RNA-seq data. Uniformly
71 processed gene counts were obtained from the GREIN platform[13]. After quality filtering (see Methods),
72 58% of the samples were kept, corresponding to 2.705 samples from 62 studies and comprising 45
73 diseases (Supplementary Data 1).

74 We performed differential expression analyses to obtain significantly differentially expressed genes
75 (sDEGs) for each disease (see Methods, Supplementary Table 1). As expected, the number of sDEGs
76 positively correlates with the sample size, whereas it does not correlate with the average library size
77 (average number of sequenced reads) of the diseases (Supplementary Fig. 1).

78 To better understand the transcriptomic alterations associated with the analyzed diseases, we performed
79 functional enrichment analyses[14] and, focusing on the significantly enriched Reactome pathways
80 (FDR<=0.05)[15], we clustered diseases based on their binarized Normalized Effect Sizes (see Methods,
81 Fig. 1 and Supplementary Fig. 2-4).

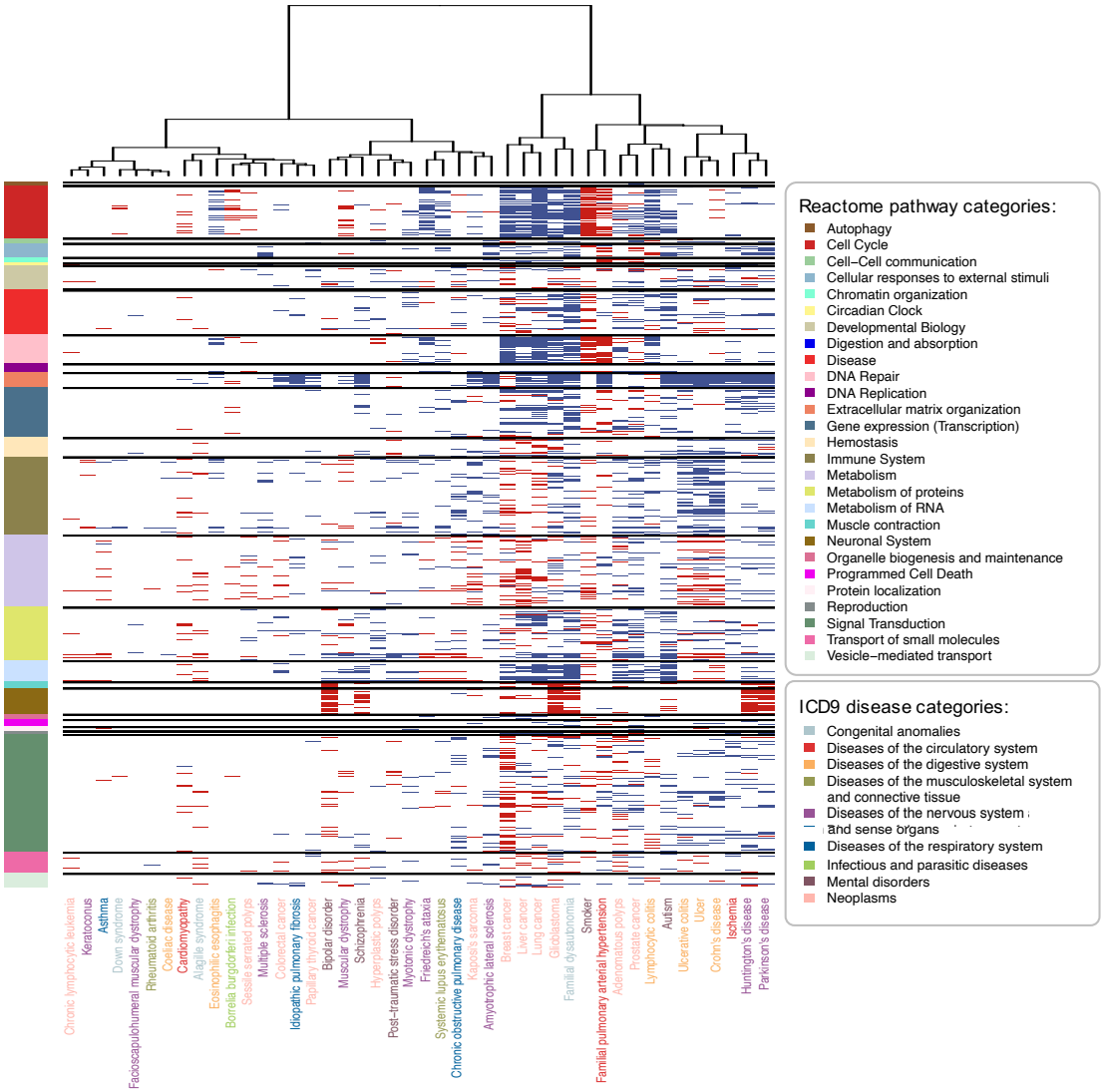

Fig. 1. Reactome pathways significantly dysregulated in human diseases grouped by pathway category. For each disease, Reactome pathways significantly up- and down-regulated were identified using the GSEA method (FDR <= 0.05). Ward2 algorithm was applied to cluster diseases based on the Euclidean distance of their binarized Normalized Effect Size (1s, and -1s for up- and down-regulated pathways). The heatmap shows the dysregulated Reactome pathways (rows) in the diseases (columns), where up- and down-regulated pathways are blue and red colored respectively. Reactome pathways are sorted and grouped by pathway categories (separated by black horizontal lines). Diseases are colored by ICD9 disease category. Diseases with 0 dysregulated pathways are not shown.

When considering the pathway enrichment (Fig. 1), two main clusters are defined, one containing less enriched pathways than the other. Most ICD9 disease categories have diseases distributed across the branches, pointing to the involvement of some specific shared biological processes in their pathology. Among others, neuronal system- and extracellular matrix (ECM) organization-related pathways are

over and underexpressed respectively in mental and nervous system disorders (bipolar disorder, schizophrenia, Huntington's disease (HD), Parkinson's disease and autism), as previously described in the literature[16,17]. On the other hand, most neoplasms present the expected overexpression of pathways related to the cell cycle, DNA repair, DNA replication, ECM, as well as a decreased hemostasis. Nonetheless, alterations related to developmental biology, immune system and signal transduction are generally observed in specific cancer types[18–20].

Moreover, diseases of the digestive system like the Inflammatory Bowel Diseases (IBD): Crohn's disease and ulcerative colitis, as well as the closely related lymphocytic colitis and ulcer, present an overexpression of a broad set of immune system-related pathways (Supplementary Fig. 2a). Specifically, ulcerative colitis, Crohn's disease and ulcer form a distinct cluster and share pathways mainly related to cell-cell communication, hemostasis, metabolism, and signal transduction (Supplementary Fig 2b-d and 3a). A common overexpression of multiple specific pathways regarding the ECM organization is observed in IBD (Supplementary Fig. 4c), recently described not only as a consequence of the *in situ* inflammation but also as an active mediator of it[21]. Among other pathways, ECM processes are also observed and described to be altered in diseases for which IBD is a risk factor, such as ulcer and colorectal cancer[22,23].

Disease similarity network

Next, we built a disease similarity network (DSN) connecting diseases based on the Spearman's correlation (FDR<=0.05) of the genes in the union of their sDEGs (see Methods, Fig. 2). The network is composed of one single connected component - 63.37% positive interactions, 36.63% negative interactions - with a mean degree of 29.24 (Supplementary Table 2, Supplementary Fig. 5, see Methods). Nodes' degree positively correlates with the number of sDEGs and the sample size of the diseases (Supplementary Fig. 6).

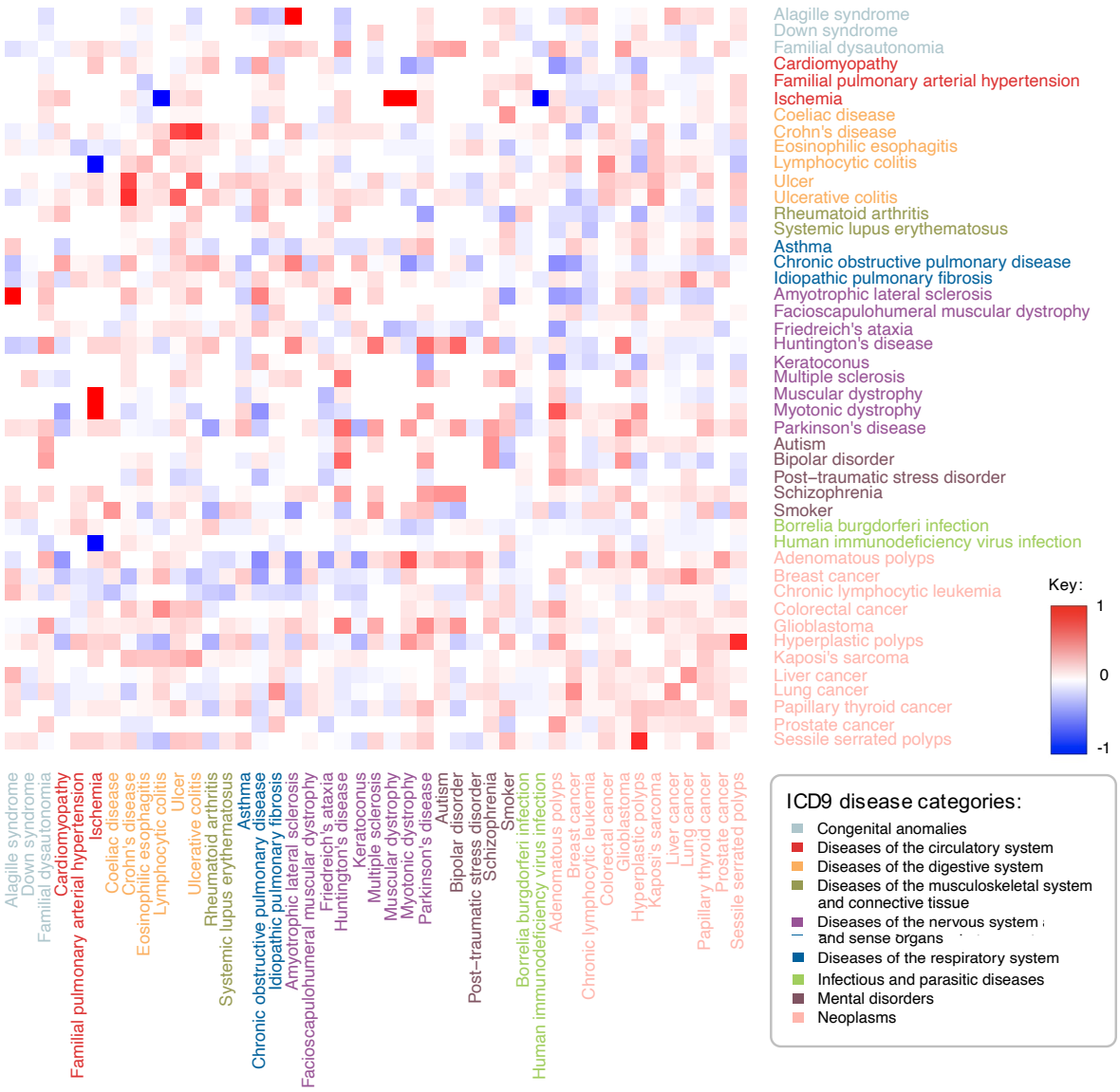

Fig. 2. Heatmap representation of the disease similarity network. Pairwise disease correlations were computed based on the Spearman's correlation of the union of the sDEGs of each pair of diseases. A disease-disease network was built, containing the significantly positive and negative correlations (FDR <= 0.05), where the edge weights in the network correspond to the Spearman's correlations (see Methods). The heatmap shows the network's positive and negative disease interactions, in red and blue respectively. White represents pairs of diseases that are not connected. Diseases are colored by ICD9 disease category.

The DSN captured the previously described IBD comorbidities, as well as intra-disease category comorbidities regarding neoplasms (e.g. lung and liver cancer). We also observed a positive correlation between the differential expression profiles of Kaposi's sarcoma (KS) and human immunodeficiency virus' infection (HIV), being this neoplasm one of the most common malignancies in HIV patients as a

132 consequence of their immune deficiency[24]. We also captured a previously described less frequent link
133 between KS and other diseases characterized by an immune system imbalance, such as IBD[25,26].

134 Many positive interactions entailing diseases of the nervous system and mental disorders are observed,
135 mainly due to shared neurological dysfunction, ECM dysregulation and, in some cases, immune system
136 involvement (Fig. 1 and 2). Among others, schizophrenia was found to be connected to bipolar disorder,
137 autism, and Parkinson's and Huntington's diseases, which are known to be comorbid.

138 Additionally, we observed some negative correlations between the expression profiles of specific
139 central nervous system disorders (CNSd) and cancers[27]. For instance, HD presents negative correlations
140 with liver, lung, and breast cancer and chronic lymphocytic leukemia, which are known to co-occur less
141 than the expected by chance[28]. When comparing the altered pathways for both diseases, we find opposite
142 molecular tendencies in multiple of their key pathogenic processes. On one hand, cancer is characterized
143 by an overexpression of cell cycle and gene transcription processes, whereas HD shows increased cell
144 death, apoptosis, mitochondrial dysfunction and a negative regulation of gene expression
145 (Supplementary Fig. 3c-d, 2c and 4a). Kinesins-related pathways, involved in cell division and
146 intracellular transport, are overexpressed in cancer as previously described[29], and underexpressed in
147 HD, where its impairment is also characterized[30] (Supplementary Fig. 2c). Additionally, immune
148 abnormalities have been extensively described as central to HD and cancerous processes[31,32]. For
149 instance, we observed an increased interleukin production and signaling regarding Th1-type immune
150 response (e.g. IL-12) in HD, as well as an activation of the complement cascade, being both processes
151 underexpressed in cancer and previously linked to carcinogenesis[31–33] (Supplementary Figure 2a).

152 Subsequently, we evaluated to what extent the DSN is able to capture medically known comorbidities
153 by computing its overlap with the epidemiological network from Hidalgo *et al*[2]. We observed that the
154 DSN significantly overlaps 46.2% of the interactions in Hidalgo *et al.*[2] over the common set of diseases
155 (p-value = 0.0018) (Supplementary Table 3, see Methods). We also showed that the overlap of the
156 negative interactions was not significant (p-value = 0.867). The DSN precision and recall varies
157 depending on the disease category pair (Fig. 3a). For instance, diseases of the digestive system present
158 the highest precision (66.4%) with a mean recall of 53.6%. Interactions entailing congenital anomalies
159 are also captured at a high level. On the contrary, highly heterogeneous diseases (e.g. mental disorders)
160 tend to present lower recall values and neoplasms, which often share the dysregulation of multiple
161 pathways without being comorbid, exhibit the lowest precision.

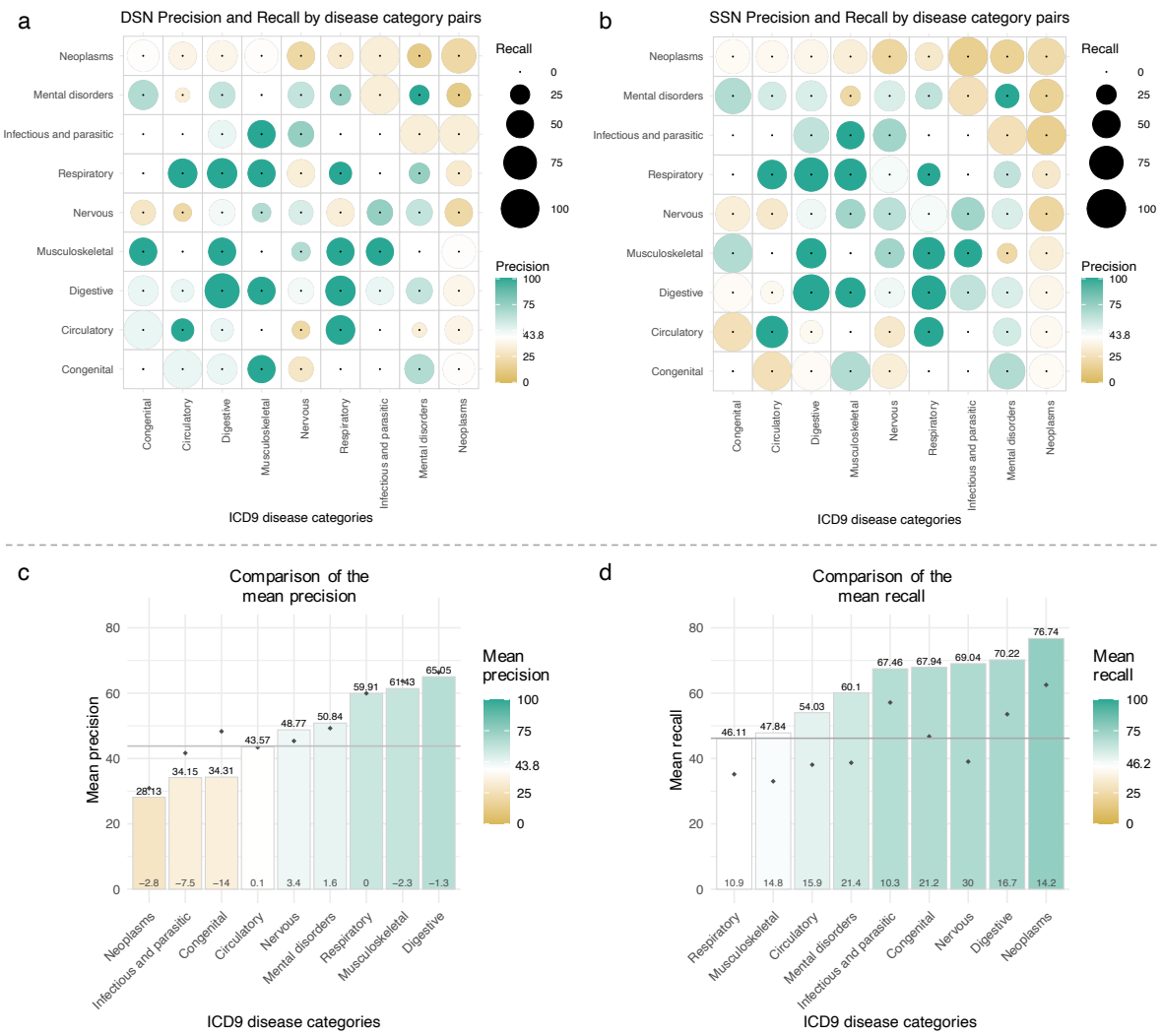

Figure 3. Precision and recall of the DSN and SSN by disease category. Precision and recall of the (**a**) Disease Similarity Network (DSN) and the (**b**) Stratified Similarity Network (SSN) by disease category pairs. The precision is the percentage of interactions in the molecular networks present in the epidemiological network from Hidalgo *et al.*[2] and the recall is the percentage of epidemiological interactions captured by the molecular networks. For the SSN, interactions between meta-patients and diseases were considered (See Methods). Each point in the symmetric matrix corresponds to the subnetwork that results from selecting the interactions between diseases of the indicated disease categories. The area of the circles represents the recall and the color corresponds to the precision. Green and yellow colors indicate higher and lower precisions than the one of the DSN (43.8%), represented in white. Disease pairs without epidemiological interactions present a single black point. **(c)** Mean precision of each disease category in the SSN. Disease categories are sorted by their mean precision. Green and yellow colors indicate higher and lower precisions than the one of the DSN, represented in the horizontal grey line. **(d)** Mean recall of each disease category in the SSN. Disease categories are sorted by their mean recall. Green and yellow colors indicate higher and lower recalls than the one of the DSN (46.2%), represented in the horizontal grey line. Black points indicate the mean **(c)**

177 precision or **(d)** recall of the disease categories in the DSN. The differences between the values at the meta-
178 patient and disease level are plotted in the base of the bars.
179
180 Moreover, we studied the topological properties of the molecular and epidemiological networks
181 (Supplementary Table 4). Both networks contain one single connected component that comprises all
182 the diseases, being the DSN denser. The DSN composed only of positive interactions and the
183 epidemiological network present a transitivity around 0.5, meaning that nodes connected to a third one
184 have 0.5 probability of being connected. Also, both networks present a mean distance below 2,
185 indicating a high connectivity. Then, we compared the topological properties of the positive ICD9-
186 based DSN subnetwork and the epidemiological network, considering only the common set of diseases
187 (Supplementary Table 5). We observe that both subnetworks have a very similar global topology. For
188 instance, they present a significantly equal mean degree and a very similar density and mean distance
189 (slightly higher for the epidemiology) around 0.42 and 1.6 respectively. Although both networks have
190 a similar mean transitivity above 0.5, it is significantly higher for the epidemiological network, possibly
191 due to other forces such as common risk factors or lifestyle. The networks also present a significantly
192 equal mean closeness, betweenness and degeneracy. Finally, we computed the assortativity of the
193 networks labeling the nodes with their ICD9 disease category. We found that both networks present an
194 assortativity around 0; the epidemiological network is slightly depleted in within-category disease links
195 whereas the DSN seems to present a minimal enrichment in those.
196 Next, we compared our overlap with the ones derived from published disease-disease networks based
197 on other molecular data (see Methods). Both the microbiome[10] and the miRNA[9] networks yielded non-
198 significant overlaps with the epidemiological network over their respective common diseases and over
199 the common diseases also present in the DSN. The network derived from protein-protein interaction
200 (PPI) networks presented significant yet small overlaps with the epidemiology (8.71% for the entire
201 network and 18.52% over the diseases in the DSN), and the one generated by Sánchez-Valle *et al.*[8]
202 using microarrays presents a significant overlap of 16% with the epidemiological network from Hidalgo
203 *et al.*[2] (Fig. 4a and Supplementary Table 6).
204 Finally, we compared the networks that present a significant overlap with the epidemiology (PPI and
205 microarray-based networks) with the DSN (Supplementary Table 7-8). The network derived from PPIs
206 and the DSN share 19 ICD9 codes and only 6 out of the 20 interactions present for these diseases in the
207 former are found in the later (there is no significant overlap between them) (Supplementary Table 7-8).
208 Between these common diseases, 29 epidemiologically known comorbidities are connected only in the

DSN whereas 10 are unique to the other network (Fig. 4b). The entire DSN provides information for 22 new ICD9 codes and uniquely captures 149 disease links described in the epidemiology.

On the other hand, the microarrays' network contains 92 ICD9 codes, where 27 of them are analyzed in the DSN. We computed the overlap of both networks over the common set of ICD9 codes, yielding a significant overlap (p-value = 0.027) of 47.02% of the microarrays' network. Specifically, positive interactions have a significant overlap (p-value = 0.002) of 62.22% whereas the overlap of the negative interactions is not significant (p-value = 0.624) (Supplementary Table 8). Among these common diseases, the DSN yielded 42 new positive interactions that are described in the epidemiological network by Hidalgo *et al.*[2] (e.g. Crohn's disease and ulcerative colitis) (Fig. 4c). Additionally, the DSN provides information for 14 new ICD9 codes and captures 141 new interactions that match known comorbidities.

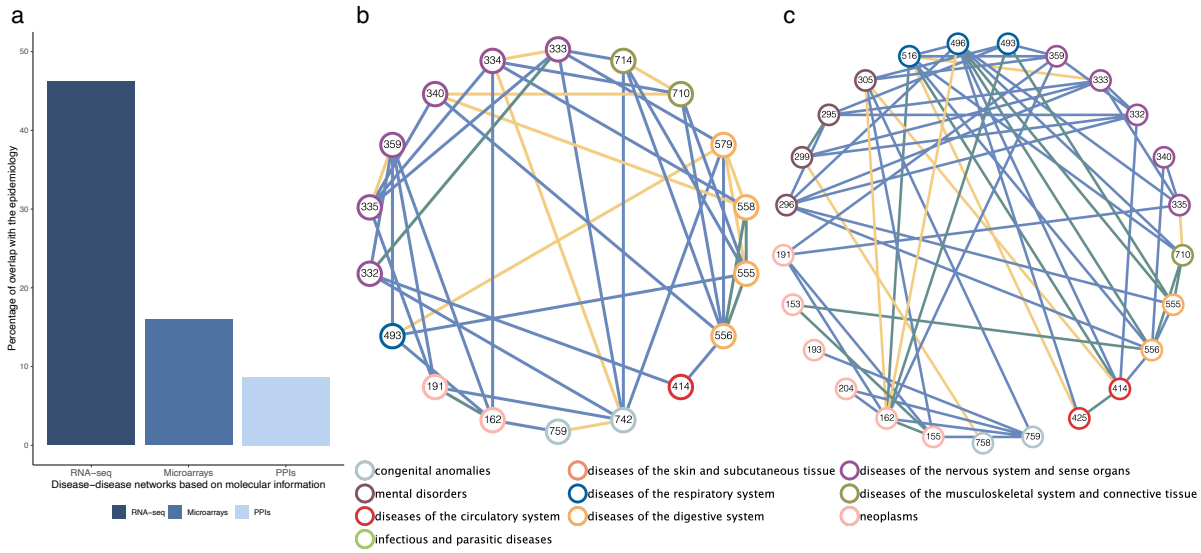

Figure 4. Comparison of the epidemiological interactions described in the Disease Similarity Network (DSN) and other disease-disease networks based on molecular information. (a) Percentages of interactions in the epidemiological networks, significantly captured by molecular networks. It shows the overlap of our DSN based on RNA-seq and the networks based on microarrays and protein-protein interactions (PPI) (See Methods). **(b)** Network visualization of the positive disease-disease interactions described in the epidemiological network by Hidalgo *et al.*[2] that captured only by the DSN (blue), only by the network based on PPIs[6] (yellow) or by both of them (green). It shows the interactions over the common set of ICD9 codes in both molecular networks. Diseases are colored by their ICD9 code category. **(c)** Network visualization of the positive disease-disease interactions described in the epidemiological network

231 by Hidalgo *et al.*[2] that captured only by the DSN (blue), only by the DMSN based on microarrays[8] (yellow)
232 or by both of them (green).
233

234 **Molecular mechanisms behind comorbidities**

235 Once confirmed that the DSN captures a significant percentage of comorbidities, we inspected which
236 are the molecular mechanisms underlying its epidemiological (EIs) and non-epidemiological
237 interactions (NEIs), i.e. interactions for which it was not possible to find a correspondence with the
238 current medical data. We observe that the Reactome pathway categories behind most interactions tend
239 to display a wider range of dysregulation than those affected only in some interactions; i.e. they share
240 a higher number of altered pathways (Fig. 5). Impressively, 95.2% of the EI in the DSN share at least
241 one -and a mean of 21.2- overexpressed immune system pathways, followed by pathways related to the
242 ECM, metabolism of proteins, metabolism and signal transduction, all involved in over 90% of the
243 interactions (means = 10.9, 10.1, 6.3, 16.1). The underexpressed pathways involved in most of the EIs
244 are related to the metabolism of proteins, signal transduction, metabolism, and developmental biology
245 (means = 4.9, 7.2, 13.5, 2.5).

246 To adequately detect which pathways are specific to EI, we also take into account the ratio between the
247 mean number of shared over or underexpressed pathways by Reactome category in EIs versus NEIs
248 (Fig 5, Supplementary Fig. 7). Overexpressed circadian clock pathways explain more EIs than NEIs,
249 being the mean number of shared pathways 1.7 times higher in the former than in the latter. Digestion
250 and absorption and protein localization are 3.8 and 1.6 times more commonly underexpressed in the
251 EIs.

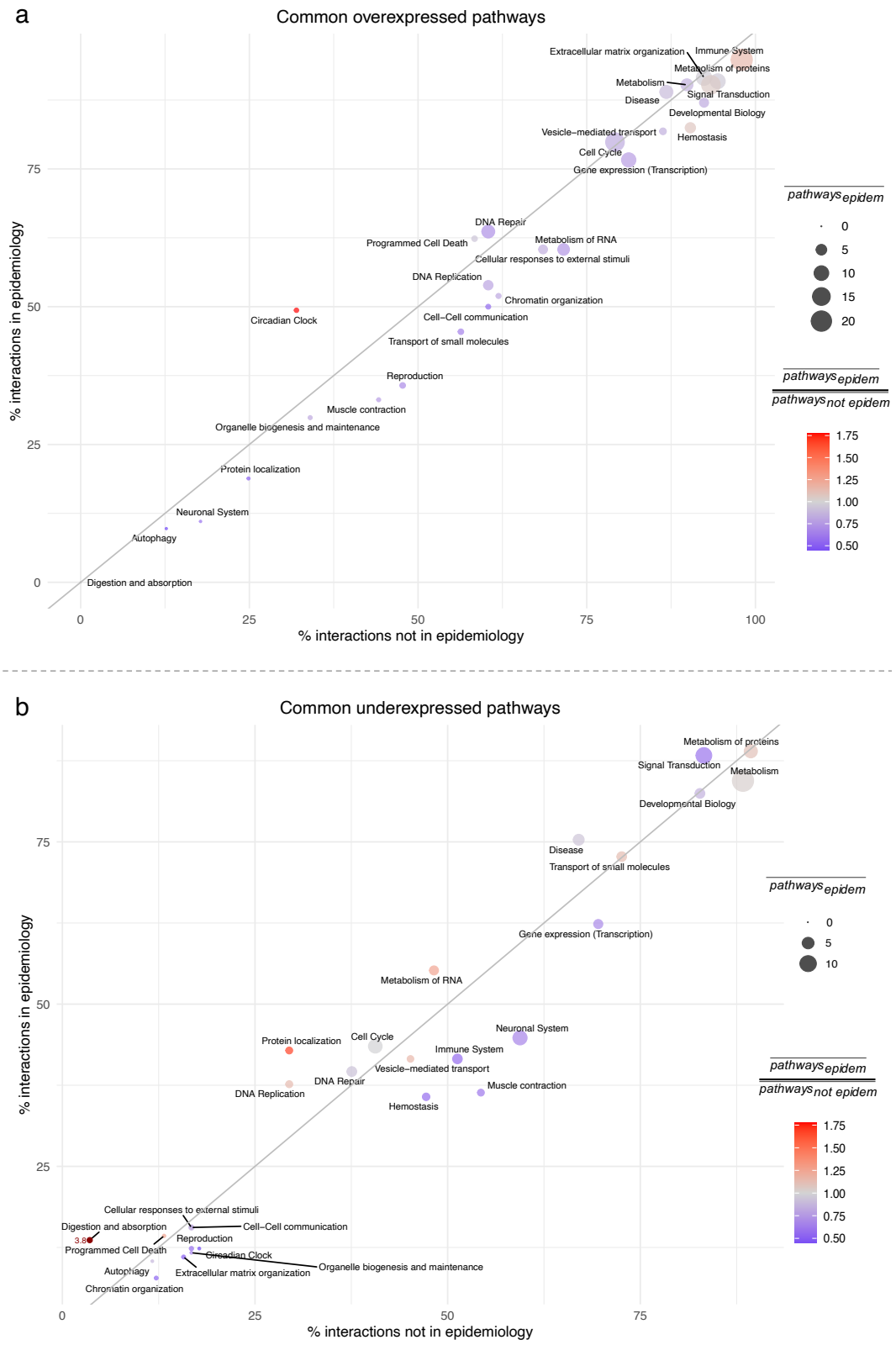

Figure 5. Over and underexpressed pathways behind epidemiological and non-epidemiological interactions. Percentage of epidemiological versus non-epidemiological interactions that share **(a)** overexpressed or **(b)** underexpressed pathways. Each point represents a Reactome pathway category. The size of the points corresponds to the mean number of shared pathways in the epidemiological interactions.

257 The color corresponds to the ratio of the mean number of shared pathways in epidemiological versus non-
258 epidemiological interactions (e.g. red indicates that epidemiological interactions share more altered
259 pathways than non-epidemiological interactions).
260
261 Higher resolution results can be obtained by considering interactions between pairs of disease
262 categories. For instance, the shared overexpression of circadian clock pathways seems to be highly
263 specific of EIs entailing CNSd (Fig. 5 and 6a). Actually, the pivotal and putatively causal role of the
264 circadian system in CNSd and their comorbidities has recently been proposed[34–36]. Although each
265 individual comparison has its particular portrait of the mechanisms underlying disease interactions,
266 some general patterns become apparent. We observe that pathways tend to cluster according to their
267 ability to explain EI versus NEIs. In Fig. 6a we can see a cluster of pathways whose dysregulation is
268 shared by all EIs whereas smaller clusters are mostly present in NEIs. Interestingly, pathway categories
269 involved in more EIs than NEIs also present a higher number of pathways commonly dysregulated in
270 EIs than in NEIs (Fig. 6a, within the upper cluster, redder dots are observed at the left side). In summary,
271 EIs have been found to present more shared altered pathways than NEIs. In fact, if we remove
272 neoplasms, EIs share the alteration of 53.1% and 56.8% more over and underexpressed pathways,
273 respectively. Nonetheless, by inspecting the interactions between neoplasms, we can discern between
274 the mechanisms that are potentially responsible for their common cause from the ones that are more
275 likely due to the convergence of some common functions (i.e. overexpression of pathways related to
276 the immune system or cell-cell communication as well as the underexpression of developmental biology
277 or DNA repair processes) (Fig. 6b and Supplementary Fig. 8). Comorbid neoplasms tend to share a
278 higher number of overexpressed pathways related to organelle biogenesis and maintenance, chromatin
279 organization or cell cycle and an underexpression of pathways such as: metabolism, transport of small
280 molecules or the immune system. Interestingly, around 30% of comorbidities within neoplasms share a
281 highly specific overexpression of protein localization pathways.

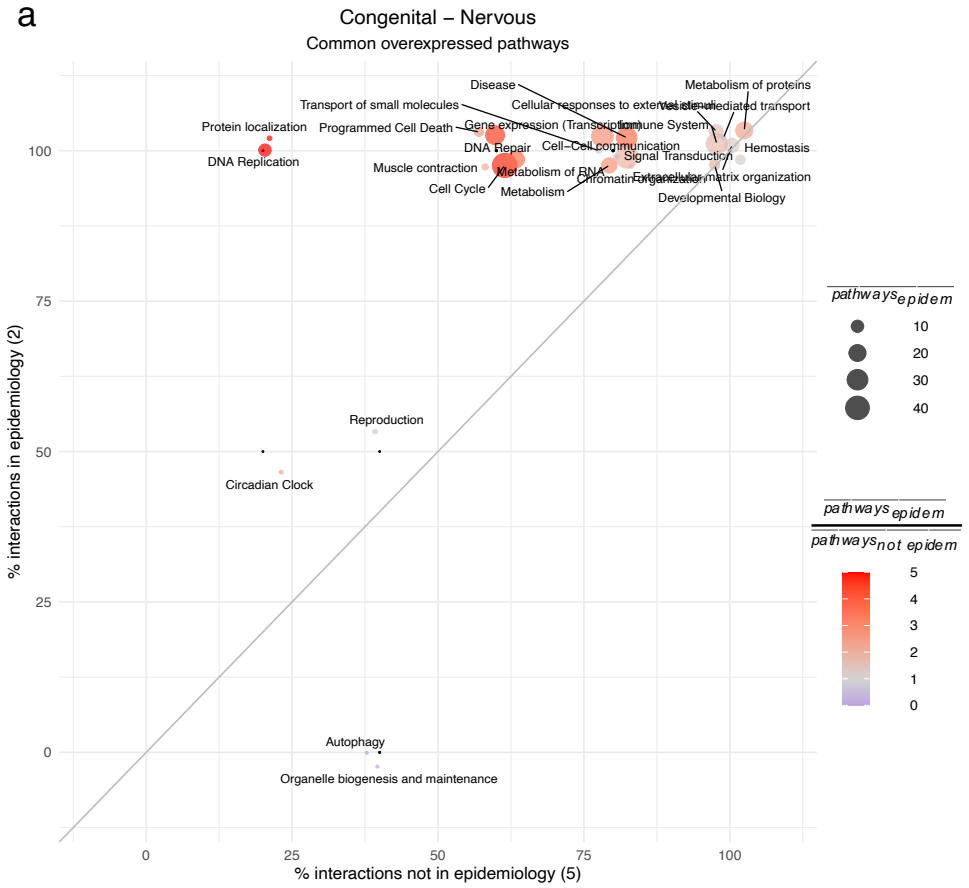
a
Congenital – Nervous
Common overexpressed pathways
Disease
Metabolism of proteins
Transport of small molecules
Cellular responses to external stimuli
Vesicle-mediated transport
Protein localization
Programmed Cell Death
Gene expression (Transcription)
Immune System
DNA Repair
Cell–Cell communication
Hemostasis
DNA Replication
Muscle contraction
Signal Transduction
Metabolism of RNA
Chromatin organization
Extracellular matrix organization
Cell Cycle
Metabolism
Developmental Biology
Reproduction
Circadian Clock
Autophagy
Organelle biogenesis and maintenance
% interactions in epidemiology (2)
% interactions not in epidemiology (5)
0
25
50
75
100
pathways epidem
10
20
30
40
pathways epidem / pathways not epidem
5
4
3
2
1
0

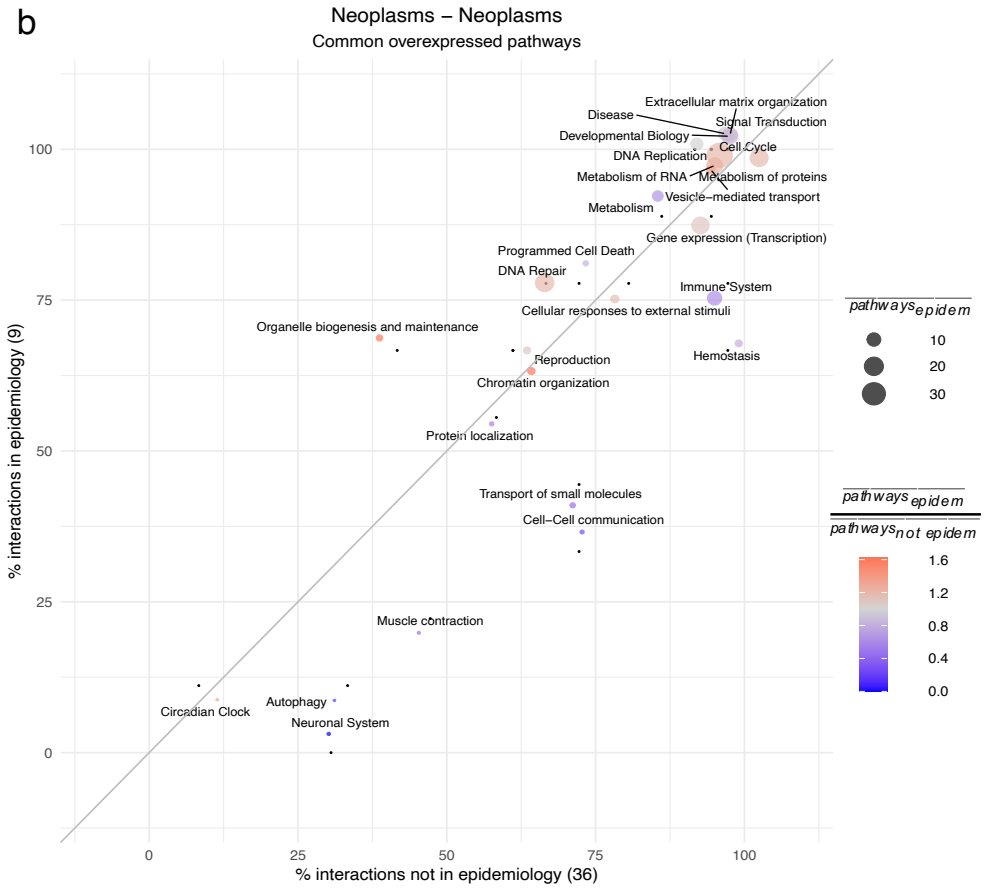
b
Neoplasms – Neoplasms
Common overexpressed pathways
Extracellular matrix organization
Disease
Signal Transduction
Developmental Biology
Cell Cycle
DNA Replication
Metabolism of RNA
Metabolism of proteins
Vesicle–mediated transport
Metabolism
Gene expression (Transcription)
Programmed Cell Death
DNA Repair
Immune System
Cellular responses to external stimuli
Organelle biogenesis and maintenance
Hemostasis
Reproduction
Chromatin organization
Protein localization
Transport of small molecules
Cell–Cell communication
Muscle contraction
Circadian Clock
Autophagy
Neuronal System
% interactions in epidemiology (9)
% interactions not in epidemiology (36)
0
25
50
75
100
pathways epidem
10
20
30
pathways epidem / pathways not epidem
1.6
1.2
0.8
0.4
0.0

282

283 **Figure 6. Examples of overexpressed pathways behind epidemiological and non-epidemiological**
284 **interactions.** Percentage of epidemiological (EIs) versus non-epidemiological interactions (NEIs) that share
285 overexpressed pathways. Each point represents a Reactome pathway category. The size of the points
286 corresponds to the mean number of shared overexpressed pathways in the EIs. The color corresponds to the
287 ratio of the mean number of shared pathways in EIs versus NEIs (e.g. red indicates that epidemiological
288 interactions share more pathways than non-epidemiological interactions). The number of EIs and NEIs is
289 indicated between parentheses in the y and x axis labels, respectively. (**a)** Interactions between congenital
290 anomalies and diseases of the nervous system and sense organs. (**b**) Interactions within neoplasms.
291

292 **Defining disease meta-patients**

293 It has been shown that patients suffering from a given disease often present different risks of developing
294 specific secondary conditions[4]. We hypothesize that such differential risks might be driven by the
295 existence of disease subtypes. To evaluate it, we studied disease similarities in a stratified manner by
296 applying clustering algorithms to obtain subgroups of cases with a similar expression profile for each
297 disease (see Methods). We consider those subgroups as meta-patients. To evaluate our approach, we
298 selected breast cancer, a disease with known molecular subtypes for which we have two independent
299 studies. The first study contains 20 estrogen positive (ER+) samples and 18 triple negative (TN) and
300 the second study entails 9 estrogen negative (ER-) samples and 9 ER+. Our two independently obtained
301 clusters (using PAM[37] and Ward2[38] clustering algorithms separately) yielded similar results, being PAM
302 the most accurate when grouping cases according to their defined molecular subtypes (Supplementary
303 Fig. 9 and Supplementary Table 9). Breast cancer patient's clustering and pairwise similarity shows
304 that PAM clustering classifies most of the cases correctly into estrogen negative (ER-), triple negative
305 (TN) and estrogen positive (ER+) (Fig. 7a), even grouping cases with shared molecular subtypes that
306 belong to two independent studies.

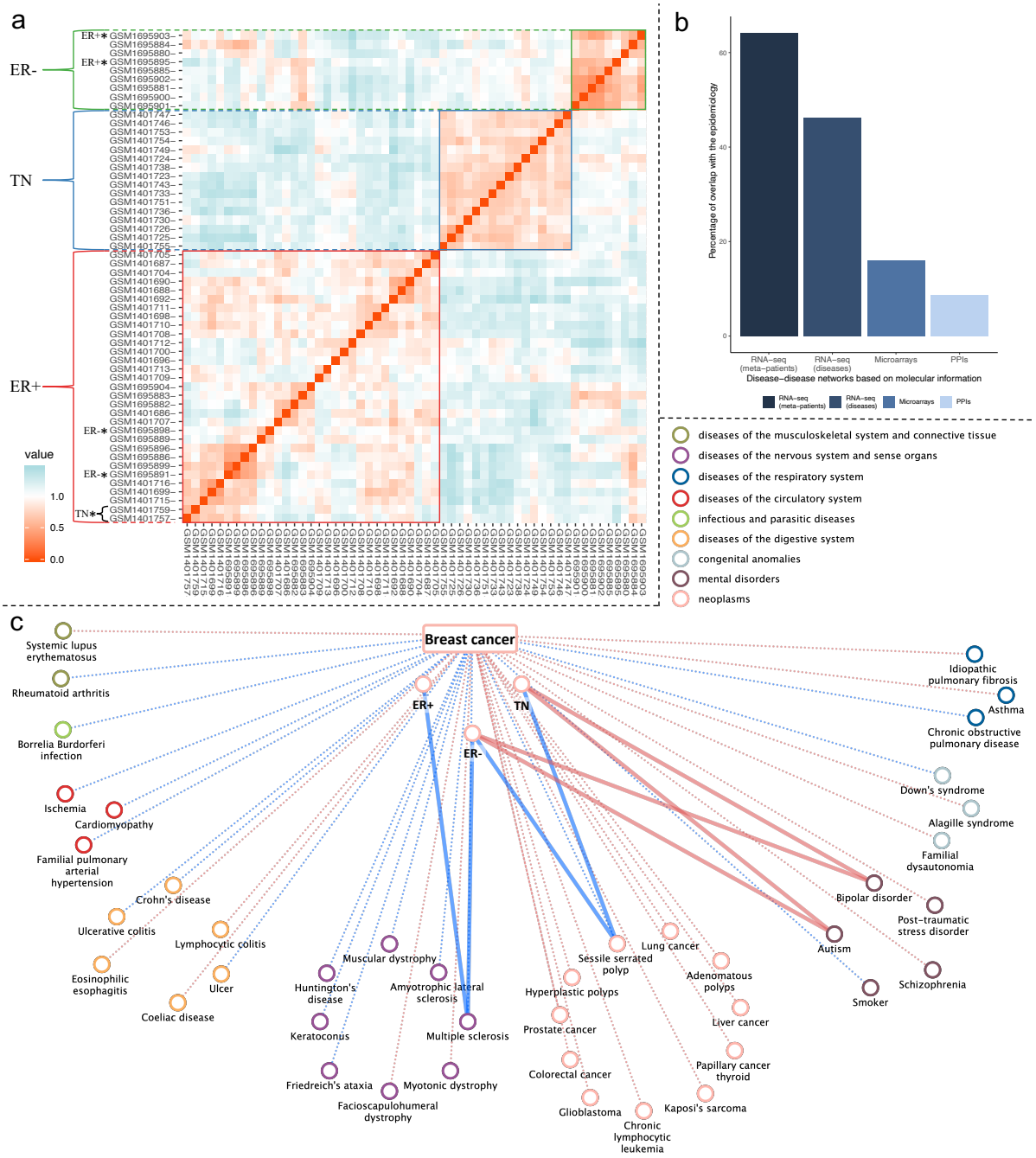

Fig. 7. Breast cancer meta-patients and breast cancer molecular similarity interactions at the disease and meta-patient level. (a) Heatmap showing breast cancer patients' similarity and classification through PAM algorithm. The similarity has been defined as 1 – Spearman's correlation of the gene expression values. Orange represents a positive correlation between the expression profile of the patients whereas blue represents a negative correlation between them. Patients are colored based on their molecular subtype. Patients are divided in 3 subtypes: ER- (Estrogen negative) in green, TNEG (Triple negative patients) in blue and ER+ (Estrogen positive) in red. Patient's clustering is marked on the left side of the figure. **(b)** Percentages of interactions in the epidemiological networks, captured by molecular networks in a significant manner. It shows the overlap of the interactions at the meta-patient and disease level based on RNA-seq and

317 the networks based on microarrays and protein-protein interactions (PPI) (See Methods). **(c)** Interactions
318 between breast cancer disease and its meta-patients with human diseases. Positive interactions are
319 represented in red and negative interactions in blue. Dashed-faded lines represent interactions at the disease
320 level and shared by all the meta-patients whereas solid lines represent meta-patient specific interactions.
321

322 **Stratified Similarity Network**

323 Since meta-patients are groups of patients from a given disease, they can be treated as any phenotype
324 to which we can apply gene expression analysis methods that assign a significance to their conclusions.
325 Hence, and first of all, we characterized the obtained meta-patients in terms of their differential
326 expression profiles (see Methods). Then, we built a network based on the gene expression similarity
327 between all the meta-patients and analyzed diseases following the methodology described for the
328 generation of the DSN (see Methods). The resulting Stratified Similarity Network (SSN) contains three
329 types of interactions: (1) the previously described disease-disease interactions, (2) interactions
330 connecting different meta-patients and (3) interactions connecting meta-patients to diseases. The SSN
331 can be fully explored in the web application (see Methods) and its topological properties can be found
332 in the Supplementary Table 4. Since the SSN has a considerably higher number of nodes, we observe a
333 large increase in mean degree with respect to the DSN. As captured by the moderate increase in density
334 and mean transitivity, the meta-patients have added some new interactions that were missed by the
335 DSN, being able to uncover new transitive relationships. These properties, along with a concordant
336 decrease in diameter and mean distance, occur across the entire network and subnetworks entailing
337 positive or negative interactions. In fact, by defining meta-patients we significantly increase the number
338 of diseases linked to each disease by 7.64 diseases (p-value=1.596e-10) and 7.29 (p-value = 6.159e-15)
339 for the positive and negative interactions respectively (Supplementary Fig. 10a). We confirmed that this
340 increase in detection power is significant compared to randomly generated meta-patients (p-value = 0
341 for positive and negative interactions) (see Methods) (Supplementary Fig. 11).

342 We inspected the links between breast cancer disease and its meta-patients with the rest of diseases (Fig.
343 7c). We observe that while most of the interactions are shared between breast meta-patients and the
344 disease, several interactions are specific to some of them. For instance, a negative interaction with
345 multiple sclerosis is only found in ER+ and ER- meta-patients while a positive interaction with autism
346 and bipolar disorder is specific to TN and ER- meta-patients.

347 While breast cancer meta-patients share most of their connections, this is not the case for all the diseases.
348 Actually, the percentage of positive and negative links shared by all the meta-patients from a given

349 disease varies greatly (Supplementary Fig. 10b). For example, CNSd (e.g. schizophrenia, bipolar
350 disorder, MS or autism), known to be highly heterogeneous, show little consistency in their meta-
351 patients' interactions. On the other hand, neoplasms - that tend to present a consistent and high alteration
352 of multiple biological processes - seem to present a higher correspondence in their meta-patients'
353 connections.

354 To evaluate the ability of meta-patients to uncover new comorbidities, we computed the overlap of the
355 interactions between meta-patients and diseases with the epidemiological data (see Methods).
356 Remarkably, meta-patients significantly captured 64.1% (p-value = 0.0187) of the interactions in the
357 epidemiological network from Hidalgo *et al.*[2], which corresponds to an increase in recall of 17.9% with
358 respect to the DSN with a very small decrease in precision of 0.7%. On the contrary, negative
359 interactions do not show a significant overlap (p-value = 0.8035) (Supplementary Table 10). As Fig. 3
360 shows, most disease categories benefit from the stratification of diseases, since they tend to present a
361 considerable increase of the recall which is usually accompanied by a slight decrease in precision.
362 Aligned with previous results, highly heterogeneous diseases (nervous system and mental disorders)
363 present some of the highest increases in recall (up to 30%); strikingly, also gaining precision. More
364 moderately, this tendency also occurs for circulatory diseases. Respiratory diseases, which often display
365 a wide range of immune system responses, present 10.9% more recall with the same precision than in
366 the DSN.

367 Finally, we developed a web application (http://disease-perception.bsc.es/rgenexcom/) in which the
368 networks and their underlying molecular mechanisms can be easily inspected (see Methods).

369

370 # Discussion

371 So far, many molecular representations of disease interactions have failed to explain a noteworthy
372 number of the medically known comorbidities, being unable to answer the long-standing question of
373 the molecular origin of comorbidities. The generated networks based on RNA-seq profiles provide a
374 convincing and comprehensive answer to this matter, being able to significantly capture and
375 meaningfully explain 64% of the known comorbidities. Hence, they render a qualitative difference over
376 previous studies, providing a solid support to the key role of molecular mechanisms behind
377 comorbidities in a generalized manner.

378 Actually, the DSN and the epidemiological network are very similar from a topological perspective.
379 They present significantly equal mean degree, closeness, betweenness and degeneracy, as well as very

380 similar density and mean distance; indicating a general resemblance in their overall structure and
381 information flow. They also show close to zero assortativities with respect to disease categories
382 (minimally negative in the epidemiology and positive in the DSN), which implies a slight tendency of
383 diseases from the same category to be linked more than expected in epidemiology. For instance, while
384 the observed molecular similarities connect some neoplasms that are indeed comorbid (e.g. liver cancer
385 with glioblastoma, lung, or colorectal cancer), they also link specific cancers that are not
386 epidemiologically linked. This evidence shows that the presence of shared molecular mechanisms does
387 not always translate into an increased relative risk that is observed in the currently limited medical data.
388 However, we can discern between the mechanisms behind well-established comorbidities from the ones
389 that may be a consequence of an overall molecular similarity, which is especially relevant for neoplasms
390 that share similar dysregulated pathways. Indeed, without considering neoplasms, EIs tend to share over
391 50% more altered pathways than pairs of diseases without clear evidence of a medical relation (NEIs).

392 Several ways in which shared molecular mechanisms can underlie direct comorbidities have been
393 proposed. Essentially, molecular mechanisms can be causally or consequentially altered in a given
394 disease; which, in turn, can contribute to the development of a secondary condition. Thus, molecularly
395 based comorbidities can be explained by the following scenarios: (1) both diseases share the same or
396 correlated causal alterations, (2) the molecular mechanisms altered as a consequence of one disease are
397 associated to the second condition or (3) there is a third condition that increases the risk of developing
398 both of them[1]. These schemes are not mutually exclusive and can be combined in complex manners. In
399 fact, the study of direct comorbidities in longitudinal studies has shown disease trajectories that can be
400 explained by an underlying aggravation and accumulation of specific molecular processes, especially
401 in a chronic manner[39]. This is the case for the discussed progression of IBD into colorectal cancer[40] and
402 for the highly prevalent disease trajectory that has recently been called metabolic syndrome, including
403 obesity, insulin resistance, diabetes, cardiovascular disease or even cancer[41]. These observations
404 supported the central role of the underlying molecular mechanisms in the study of individual diseases
405 and disease comorbidities, to the point where efforts have already been destined to redefining diseases
406 by incorporating both their clinical features and molecular profiles[42].

407 Comorbidity relationships can be better understood if disease subtypes and patient-specific patterns are
408 taken into account[4]. Indeed, previous epidemiological studies have identified comorbidities that depend
409 on the disease subtype[43–45]. In line with this, we introduced the concept of meta-patients and the
410 stratified exploration of their molecular similarities with diseases. The definition of meta-patients
411 unraveled a significant mean of around 14 new subgroup-specific disease connections per disease,

412 increasing the detection power of disease similarities (Supplementary Fig. 10a). This subclassification
413 of diseases based on similarities of the patients' gene expression profiles can be related to
414 epidemiological observations of comorbidities that depend on patients' characteristics. In the case of
415 breast cancer, we observed that although the three meta-patients share most of the disease interactions,
416 some specific and interesting ones emerge. For instance, TN and ER- meta-patients are the only ones
417 presenting a positive interaction with autism and bipolar disorder (Fig. 7c). While several studies[46,47]
418 have found no significant correlations, recent molecular and epidemiological evidence suggests cancer
419 as a comorbidity of autism[48,49]. Besides, an enhanced cancer risk has been described for bipolar disorder
420 patients in both genders, being the risk for breast cancer higher but non-significant[50]. Additionally, we
421 observed a negative interaction between breast cancer, ER+ and ER- meta-patients with multiple
422 sclerosis (Fig. 7c). Again, opposite tendencies are described in the literature for this connection, where
423 the order of appearance of the disease seems to drive the comorbidity pattern. It has been shown that
424 breast cancer patients are 45% less likely to develop multiple sclerosis[51]. On the other hand, multiple
425 sclerosis patients have been shown to have a significantly increased risk of breast cancer, presumably
426 driven by immunosuppression derived from the associated treatment[52]. Therefore, our analysis provides
427 new evidence on subgroup-specific comorbidities with a potential molecular explanation. Moreover,
428 we showed that the percentage of recapitulated epidemiological interactions increased from almost half
429 to 64.1% when considering the interactions between diseases and meta-patients, with a slight decrease
430 in precision of 0.7%.

431 As shown, the generated networks provide the first systematic translation of disease comorbidities into
432 molecular patterns. Previous efforts based on disease-associated genes in a PPI network were limited
433 by the incompleteness of the interactome and the biased knowledge of disease-associated genes for
434 highly studied diseases[6]. Furthermore, networks based on other molecular sources such as the
435 microbiome[10] and miRNAs[9] do not overlap epidemiological interactions significantly.

436 There are at least three factors that allowed us to significantly improve the explainability of known
437 comorbidities captured with gene expression information. First, the better quality and coverage of RNA-
438 seq data, that unbiasedly increases the number and quality of features whose similarity can be compared
439 between diseases. Secondly, an improved methodology based on the existence of a significant
440 correlation between the differential gene expression profiles of each disease pair. As a result, our disease
441 links are robust, stable and independent of the rest of diseases, even if the disease universe changed;
442 contrary to previous attempts based on relative molecular similarities, where disease links depended on
443 the rest of the network[8]. Finally, the stratification of diseases into subgroups of cases named meta-

444 patients. Opposite to patient-centric approaches, meta-patients can be methodologically treated as
445 phenotypes are handled in gene expression studies; thus, a significance can be associated to their altered
446 genes, pathways and, importantly, disease interactions in the SSN.

447 Still, there are a number of issues that, if addressed, could improve the quality of the results and the
448 coverage of the comorbidity space. First, the generated networks contain both positive and negative
449 interactions potentially representing direct and inverse comorbidities. While it is possible to validate
450 the positive ones, it is more difficult to validate the less abundant - but equally interesting- negative
451 ones (36.63%) since they are not systematically described in large studies and are only sporadically
452 addressed in the literature[53]. Nonetheless, we detected known inverse comorbidities such as: HD and
453 specific cancer types or Parkinson's disease and rheumatoid arthritis[54]. Therefore, a current limitation
454 in this study is the lack of epidemiological networks entailing inverse comorbidity relationships.

455 Another limitation is the lack of sample information, such as age, sex, or treatments, which may drive
456 transcriptomic differences between patients. Also, our samples belong to published studies focused on
457 a specific disease in a given tissue (e.g. brain, liver or blood). Since we have cases and controls for each
458 study and disease, we were able to correct for the tissue effect when generating sDEGs at the disease
459 and meta-patient level. However, it would be optimal to have comprehensive data sets of diseases from
460 the same tissue or an array of interesting tissues. Moreover, better defined and annotated disease
461 subgroups as well as their differential comorbidities could help us refine the definition of meta-patients
462 and increase their power to capture their epidemiological associations. We observed that patient
463 stratification is specially important for highly heterogeneous diseases. While some diseases (e.g. breast
464 cancer) showed few links specific to some meta-patients, more heterogeneous diseases (e.g. CNSd like
465 schizophrenia or bipolar disorder and immune system disorders like asthma) present a majority of meta-
466 patient specific links (Supplementary Fig. 10b).

467 Future perspectives include increasing sample size, so sex-specific disease similarities can be extracted
468 and compared to their epidemiologically described disease interactions[55]. Furthermore, the molecular
469 coverage of disease comorbidities could be improved by considering other molecular information that
470 may underlie comorbidities within an integrative approach[56]. For this, large disease cohorts comprising
471 different kinds of omics as well as clinical information would be needed. Furthermore, the obtained
472 molecular similarities could be used to guide drug repurposing and development[57].

473 In summary, we built disease similarity networks based on transcriptomic information that, for the first
474 time, capture and meaningfully explain a sizable percentage of medically known comorbidities in a
475 significant manner. This supports the idea that disease comorbidities have a strong molecular

476 component that is better captured with gene expression profiles than with other molecular sources.
477 Actually, differential gene expression profiles portray the diseases' altered state in a rich manner since
478 its signal might reflect from genetic alterations to the epigenetic influence on gene expression due to
479 internal or external factors such as treatments, contaminants or lifestyle.

480 This study shed light into the biological processes underlying known disease comorbidities, leading to
481 a better understanding of the molecular profile and etiology of diseases and their comorbidity
482 relationships. Importantly, although we showed that many of these mechanisms have already been
483 validated experimentally, our efforts propose numerous key genes and pathways that are still to be
484 explored. Thus, we focused our discussion on some examples and provided the molecular
485 characterization of all the diseases and meta-patients at the different levels of granularity (genes and
486 pathways) within a framework that allows for the comparison of the molecular profiles for direct and
487 inverse comorbidities in a detailed and user-friendly manner (http://disease-
488 perception.bsc.es/rgenexcom/).

489 Finally, our study stresses the need to integrate the study of disease comorbidities and their underlying
490 molecular similarities within a personalized medicine scope, with the aim to capture those disease
491 interactions that might depend on the disease subtype or other patient-specific factors. This would allow
492 us, not only to better understand the putative secondary conditions of specific patients, but to better
493 characterize the underlying molecular processes that might explain those relationships.

494

495 # Methods

496 **Gene Expression Analysis**

497 Uniformly processed RNA-seq gene counts were downloaded from the GREIN platform[13] for 72 human
498 diseases analyzed by 107 studies, including a total number of 4.267 samples.

499 An RNA-seq pipeline destined to the parallel processing of a collection of RNA-seq studies for a given
500 set of diseases was developed (Supplementary Fig. 12). First, samples with a percentage of aligned
501 reads to the genome lower than 70% were removed, as well as studies with less than 3 cases (from now
502 on patients) and control samples meeting the mentioned requirement. Secondly, and in order to perform
503 the analysis at the disease level, gene counts and metadata for each disease were integrated (only studies
504 with the disease, tissue and disease state information were considered). We performed quality controls
505 using the edgeR pipeline[58] and we applied within-sample normalization by considering the logarithm
506 of the counts-per-million (log2CPM). Afterwards, we filtered out lowly expressed genes (those with

507 less than 1 log2CPM in more than 20% of the samples) and we applied between-sample normalization
508 using the trimmed mean of M values (TMM) method[59]. After performing batch effect identification, we
509 used the limma pipeline[60] for differential expression analysis. Specifically, we built a model considering
510 sample type (case vs. control) as our outcome of interest and adjusting for the study effect, as it is the
511 most descriptive independent variable (tissue, platform and others depend on the study of origin). Genes
512 with an FDR <=0.05 were considered significantly differentially expressed genes (sDEGs). Moreover,
513 we used Combat[61] and QR Decomposition[60] batch effect removal methods to check the clustering of
514 the samples with t-Distributed Stochastic Neighbor embedding (tSNEs)[62].

515 **Functional enrichment analysis**

516 In order to better characterize the molecular processes underlying the analyzed diseases, we performed
517 Gene Set Enrichment Analyses (GSEA)[14] on the ranked lists of genes based on the differential
518 expression -log Fold Change (logFC)- results using annotations from Reactome[15], Kyoto Encyclopedia
519 of Genes and Genomes[63] and Gene Ontology[64]. We considered gene sets and pathways with an FDR
520 <= 0.05 to be significant.

521 To facilitate the interpretation of the molecular processes altered in diseases and potentially involved in
522 disease comorbidity relationships, we selected the Reactome pathways[15] significantly enriched in each
523 disease and applied Ward2 algorithm[38] to cluster diseases based on the Euclidean distance of their
524 binarized Normalized Effect Sizes (1s and -1s for up- and down-regulated pathways) (Fig. 1).

525 **Disease similarity network**

526 To define disease-disease similarities we computed, for each disease pair, the Spearman's correlation
527 between the logFC values of the genes in the union of their sDEGs. We kept the interactions between
528 different diseases that were significant after correcting for multiple testing (FDR <= 0.05). The resulting
529 disease similarity network (DSN) contains positive and negative interactions (significantly positive and
530 negative correlations respectively).

531 Then, we evaluated the overlap of the obtained positive interactions extracted from diseases' gene
532 expression similarities with the ones described by Hidalgo *et al.*[2] (based on medical records). To do so,
533 we transformed our disease names into the International Code of Diseases, version 9 (ICD9 codes).
534 Since some diseases share the same three-digits ICD9 code (e.g. muscular dystrophy, myotonic
535 dystrophy and facioscapulohumeral dystrophy share the code 359 - muscular dystrophies and other
536 myopathies), we grouped their samples together and ran the whole analysis (gene expression analysis
537 and disease-disease network building) on them, generating an ICD9 similarity network. Next, we
538 computed the overlap as the percentage of interactions of the epidemiological network -entailing

539 common diseases- captured by the ICD9 DSN's positive and negative interactions independently. To
540 show the enrichment of our network in epidemiological interactions, we also computed the overlap in
541 the opposite direction. That is, the percentage of interactions in the ICD9 DSN contained in the
542 epidemiological network. We assessed the significance of the overlaps by shuffling the interactions
543 while preserving the degree distribution. We also computed the overlaps directly from the DSN
544 (Supplementary Notes, Supplementary Table 11).

545 Finally, we compared our overlap with the one obtained with other disease-disease networks based on
546 molecular data. We downloaded networks that link diseases based on the similarities of their
547 microbiome[10] and miRNAs[9] and we generated a disease-disease network based on protein-protein
548 interactions (PPIs) by selecting the disease pairs that present a significant overlap of their network
549 modules as described by Menche *et al*.[6]. Next, we computed their overlap with the epidemiological
550 network over their common set of diseases and over the common set that is contained in our disease set.
551 Finally, we compared the ICD9-level DSN with the networks that significantly overlap the
552 epidemiology (the network based on PPIs and the microarrays' disease molecular similarity network by
553 Sánchez-Valle *et al*.[8]).

554 **Meta-patients generation**

555 We stratified diseases into subgroups of patients with similar expression profiles (meta-patients) by
556 applying clustering algorithms to the normalized and batch effect corrected gene expression matrix.
557 Both PAM (k-medoids)[65] and Ward2[38] algorithms were applied independently (Supplementary Fig. 12).

558 In the k-medoids approach, we calculated pairwise distances as 1 - the Spearman's correlation. To
559 obtain the diseases' meta-patients, first we obtained the optimal number of clusters for each disease by
560 running k-medoids for a cluster number between 2 and 15. After that, the cluster number with the
561 highest average Silhouette value was used to obtain the final meta-patients[66].

562 To evaluate our approach, we selected breast cancer, a disease with known molecular subtypes and for
563 which we have two independent studies. We compared our two independently obtained clusters with
564 the defined disease subtypes (Supplementary Table 9).

565 **Stratified Similarity Network**

566 To analyze the disease subtype-associated comorbidities, we built the Stratified Similarity Network
567 (SSN) connecting meta-patients and diseases based on the pairwise Spearman's correlation of the union
568 of their sDEGs. First, meta-patient's gene expression analysis was performed using the same approach
569 described for the diseases, where all the samples corresponding to a given meta-patient were compared

with all the controls for the disease. Then, the SSN was built following the same methodology described for the DSN by treating meta-patients and diseases equally as phenotypes. To assess if the meta-patients increase the detection power significantly, we generated 1000 random meta-patients for each disease by shuffling the cases while maintaining the meta-patients' number and size. Next, we obtained 1000 SSNs and evaluated if the number of positive and negative interactions in the SSN could be observed by chance. To evaluate if meta-patients capture epidemiologically known associations with diseases, we selected the positive interactions between meta-patients and diseases, transformed them into ICD9 codes and computed their overlap with the epidemiological network from Hidalgo *et al.*[2], as described for the DSN. This is comparable to the available epidemiological network, that comprises interactions at the disease level by evaluating if a group of patients from a given disease is at a higher risk of developing a specific secondary condition.

Web application

To facilitate the visualization and exploration of the generated networks, we implemented a web application that displays the DSN and SSN in a dynamic manner[67]. The user can filter the networks by the type of interactions (positive or negative) and by selecting a minimum and maximum threshold for the edge's weight. Community detection algorithms (greedy modularity optimization[68] or random walks[69] can be applied to the filtered network and interactions involving specific nodes can be filtered and highlighted. Furthermore, the molecular mechanisms behind diseases and disease interactions can be easily inspected and compared.

Data Availability

The code of the experiments is available at https://github.com/beatrizurda/Urda-Garcia_et_al_2021 and the code of the web application can be found at https://github.com/bsc-life/rgenexcom. The data is publicly available (Supplementary Data 1); the raw data can be downloaded from GEO (https://www.ncbi.nlm.nih.gov/geo/) and the counts can be downloaded from the GREIN platform (http://www.ilincs.org/apps/grein/).

Acknowledgments

This work has been supported by the Ph.D. Fellowship (PRE2019-090454) and funded by the Spanish Ministry of Economics and Competitiveness (RTI2018-096653-B-I00). J.S.-V. was supported by the PhD fellowship BES-2016-077403.

601 We thank Vera Pancaldi from the Centre de Recherches en Cancérologie de Toulouse, INSERM and
602 Barcelona Supercomputing Center (BSC); Anaïs Baudot from the INSERM, Marseille Medical
603 Genetics and BSC, Jose Luis Portero Navío from Novo Nordisk; Emre Guney from Hospital del Mar
604 Medical Research Institute and Universitat Pompeu Fabra, and Marta Mele from BSC for their helpful
605 critical comments on the work.

606

607 **Contributions**

608 B.U.-G, J.S.-V., R.L. and A.V. designed all the experiments. B.U.-G. performed all the experiments
609 and developed the web application. All the authors wrote the manuscript and discussed the obtained
610 results.

611 *Conflict of Interest:* none declared.

612

613 **References**

614 1. Valderas, J. M., Starfield, B., Sibbald, B., Salisbury, C. & Roland, M. Defining comorbidity:
615 Implications for understanding health and health services. *Ann. Fam. Med.* **7**, 357–363 (2009).

616 2. Hidalgo, C. A., Blumm, N., Barabási, A. L. & Christakis, N. A. A Dynamic Network
617 Approach for the Study of Human Phenotypes. *PLoS Comput. Biol.* **5**, e1000353 (2009).

618 3. Jiang, Y., Ma, S., Shia, B. C. & Lee, T. S. An epidemiological human disease network derived
619 from disease Co-occurrence in Taiwan. *Sci. Rep.* **8**, 4557 (2018).

620 4. Jensen, A. B. *et al.* Temporal disease trajectories condensed from population-wide registry
621 data covering 6.2 million patients. *Nat. Commun.* **5**, 4022 (2014).

622 5. Goh, K. Il *et al.* The human disease network. *Proc. Natl. Acad. Sci. U. S. A.* **104**, 8685–8690
623 (2007).

624 6. Menche, J. *et al.* Uncovering disease-disease relationships through the incomplete interactome.
625 *Science.* **347**, 841 (2015).

626 7. Ibáñez, K., Boullosa, C., Tabarés-Seisdedos, R., Baudot, A. & Valencia, A. Molecular
627 Evidence for the Inverse Comorbidity between Central Nervous System Disorders and Cancers
628 Detected by Transcriptomic Meta-analyses. *PLoS Genet.* **10**, 4022 (2014).

629 8. Sánchez-Valle, J. *et al.* Interpreting molecular similarity between patients as a determinant of

630 disease comorbidity relationships. *Nat. Commun.* **11**, 2854 (2020).

631 9. Lu, M. *et al.* An analysis of human microRNA and disease associations. *PLoS One* **3**, e3420
632 (2008).

633 10. Ma, W. *et al.* An analysis of human microbe-disease associations. *Brief. Bioinform.* **18**, 85–97
634 (2017).

635 11. Hrdlickova, R., Toloue, M. & Tian, B. RNA-Seq methods for transcriptome analysis. *Wiley*
636 *Interdiscip. Rev. RNA* **8**, (2017).

637 12. Costa-Silva, J., Domingues, D. & Lopes, F. M. RNA-Seq differential expression analysis: An
638 extended review and a software tool. *PLoS One* **12**, e0190152 (2017).

639 13. Mahi, N. Al, Najafabadi, M. F., Pilarczyk, M., Kouril, M. & Medvedovic, M. GREIN: An
640 Interactive Web Platform for Re-analyzing GEO RNA-seq Data. *Sci. Rep.* **9**, 7580 (2019).

641 14. Subramanian, A. *et al.* Gene set enrichment analysis: A knowledge-based approach for
642 interpreting genome-wide expression profiles. *Proc. Natl. Acad. Sci. U. S. A.* **102**, 15545–
643 15550 (2005).

644 15. Fabregat, A. *et al.* The reactome pathway knowledgebase. *Nucleic Acids Res.* **44**, D481–D487
645 (2016).

646 16. Theocharis, A. D., Manou, D. & Karamanos, N. K. The extracellular matrix as a multitasking
647 player in disease. *FEBS J.* **286**, 2830–2869 (2019).

648 17. Barros, C. S., Franco, S. J. & Müller, U. Extracellular Matrix: Functions in the nervous
649 system. *Cold Spring Harb. Perspect. Biol.* **3**, 1–24 (2011).

650 18. Sausville, E. A., Elsayed, Y., Monga, M. & Kim, G. Signal Transduction-Directed Cancer
651 Treatments. *Annu. Rev. Pharmacol. Toxicol.* **43**, 199–231 (2003).

652 19. M. Candeias, S. & S. Gaipl, U. The Immune System in Cancer Prevention, Development and
653 Therapy. *Anticancer. Agents Med. Chem.* **16**, 101–107 (2015).

654 20. Cooper, G. M. & Hausman, R. E. *The Development and Causes of Cancer*. *The Cell: A*
655 *Molecular Approach* (Sinauer Associates, 2007).

656 21. Petrey, A. C. & De La Motte, C. A. The extracellular matrix in IBD: A dynamic mediator of
657 inflammation. *Curr. Opin. Gastroenterol.* **33**, 234–238 (2017).

658 22. Shahin, M. *et al.* Remodeling of extracellular matrix in gastric ulceration. *Microsc. Res. Tech.*
659 **53**, 396–408 (2001).

660 23. Stankevicius, V. *et al.* Extracellular matrix-dependent pathways in colorectal cancer cell lines
661 reveal potential targets for anticancer therapies. *Anticancer Res.* **36**, 4559–4567 (2016).

662 24. Hoffmann, C., Sabranski, M. & Esser, S. HIV-Associated Kaposi's Sarcoma. *Oncol. Res.*
663 *Treat.* **40**, 94–98 (2017).

664 25. Rodríguez-Peláez, M. *et al.* Kaposi's sarcoma: An opportunistic infection by human
665 herpesvirus-8 in ulcerative colitis. *J. Crohn's Colitis* **4**, 586–590 (2010).

666 26. Kilincalp, S., Akinci, H., Hamamci, M., Coşkun, Y. & Yüksel, I. Kaposi's sarcoma developing
667 in a HIV-negative Crohn's disease patient shortly after azathioprine and corticosteroid
668 treatment. *J. Crohn's Colitis* **8**, 558–559 (2014).

669 27. JA, D. Inverse association between cancer and neurodegenerative disease: review of the
670 epidemiologic and biological evidence. *Biogerontology* **15**, 547–557 (2014).

671 28. McNulty, P. *et al.* Reduced Cancer Incidence in Huntington's Disease: Analysis in the
672 Registry Study. *J. Huntingtons. Dis.* **7**, 209–222 (2018).

673 29. Rath, O. & Kozielski, F. Kinesins and cancer. *Nat. Rev. Cancer* **12**, 527–539 (2012).

674 30. DeBerg, H. A. *et al.* Motor domain phosphorylation modulates kinesin-1 transport. *J. Biol.*
675 *Chem.* **288**, 32612–32621 (2013).

676 31. Soulet, D. & Cicchetti, F. The role of immunity in Huntington's disease. *Mol. Psychiatry* **16**,
677 889–902 (2011).

678 32. Gonzalez, H., Hagerling, C. & Werb, Z. Roles of the immune system in cancer: From tumor
679 initiation to metastatic progression. *Genes Dev.* **32**, 1267–1284 (2018).

680 33. Lu, X. Impact of IL-12 in Cancer. *Curr. Cancer Drug Targets* **17**, 682–697 (2017).

681 34. Logan, R. W. & McClung, C. A. Rhythms of life: circadian disruption and brain disorders
682 across the lifespan. *Nat. Rev. Neurosci.* **20**, 49–65 (2019).

683 35. Hood, S. & Amir, S. Neurodegeneration and the circadian clock. *Front. Aging Neurosci.* **9**,
684 170 (2017).

685 36. Barandas, R., Landgraf, D., McCarthy, M. J. & Welsh, D. K. Circadian Clocks as Modulators

686 of Metabolic Comorbidity in Psychiatric Disorders. *Curr. Psychiatry Rep.* **17**, 98 (2015).

687 37. Park, H. S. & Jun, C. H. A simple and fast algorithm for K-medoids clustering. *Expert Syst.*
688 *Appl.* **36**, 3336–3341 (2009).

689 38. Murtagh, F. & Legendre, P. Ward's Hierarchical Clustering Method: Clustering Criterion and
690 Agglomerative Algorithm. **31**, 274-295, (2014).

691 39. Hu, J. X., Thomas, C. E. & Brunak, S. Network biology concepts in complex disease
692 comorbidities. *Nat. Rev. Genet.* **17**, 615–629 (2016).

693 40. Nebbia, M., Yassin, N. A. & Spinelli, A. Colorectal Cancer in Inflammatory Bowel Disease.
694 *Clin. Colon Rectal Surg.* **33**, 305–317 (2020).

695 41. Bonsignore, M. R. & Steiropoulos, P. *Metabolic syndrome*. *ERS Monograph* vol. 2015
696 (StatPearls Publishing, 2015).

697 42. Zhou, X. *et al.* A Systems Approach to Refine Disease Taxonomy by Integrating Phenotypic
698 and Molecular Networks. *EBioMedicine* **31**, 79–91 (2018).

699 43. Kibune-Nagasako, C., Garcia-Montes, C., Silva-Lorena, S. L. & Aparecida-Mesquita, M.
700 Irritable bowel syndrome subtypes: Clinical and psychological features, body mass index and
701 comorbidities. *Rev. Esp. Enfermedades Dig.* **108**, 59–64 (2016).

702 44. Tsai, F. J., Tseng, W. L., Yang, L. K. & Gau, S. S. F. Psychiatric comorbid patterns in adults
703 with attention-deficit hyperactivity disorder: Treatment effect and subtypes. *PLoS One* **14**,
704 e0211873 (2019).

705 45. Witthauer, C. *et al.* Associations of specific phobia and its subtypes with physical diseases: An
706 adult community study. *BMC Psychiatry* **16**, 16:155 (2016).

707 46. Fairthorne, J., Hammond, G., Bourke, J., Jacoby, P. & Leonard, H. Early mortality and
708 primary causes of death in mothers of children with intellectual disability or Autism spectrum
709 disorder: A retrospective cohort study. *PLoS One* **9**, e113430 (2014).

710 47. Mouridsen, S. E., Rich, B. & Isager, T. Risk of cancer in adult people diagnosed with infantile
711 autism in childhood: A longitudinal case control study based on hospital discharge diagnoses.
712 *Res. Autism Spectr. Disord.* **23**, 203–209 (2016).

713 48. Forés-Martos, J. *et al.* Transcriptomic metaanalyses of autistic brains reveals shared gene

714 expression and biological pathway abnormalities with cancer. *Mol. Autism* **10**, 17 (2019).

715 49. Kao, H.-T., Buka, S. L., Kelsey, K. T., Gruber, D. F. & Porton, B. The correlation between
716 rates of cancer and autism: an exploratory ecological investigation. *PLoS One* **5**, e9372–e9372
717 (2010).

718 50. BarChana, M. *et al.* Enhanced cancer risk among patients with bipolar disorder. *J. Affect.*
719 *Disord.* **108**, 43–48 (2008).

720 51. O'Malley, P. W., Mulla, Z. D. & Nesic, O. Multiple sclerosis and breast cancer. *J. Neurol. Sci.*
721 **356**, 137–141 (2015).

722 52. Etemadifar, M. *et al.* Cancer risk among patients with multiple sclerosis: A cohort study in
723 Isfahan, Iran. *Casp. J. Intern. Med.* **8**, 172—177 (2017).

724 53. Tabarés-Seisdedos, R. *et al.* No paradox, no progress: Inverse cancer comorbidity in people
725 with other complex diseases. *Lancet Oncol.* **12**, 604–608 (2011).

726 54. Sung, Y. F. *et al.* Reduced Risk of Parkinson Disease in Patients With Rheumatoid Arthritis: A
727 Nationwide Population-Based Study. *Mayo Clin. Proc.* **91**, 1346–1353 (2016).

728 55. Westergaard, D., Moseley, P., Sørup, F. K. H., Baldi, P. & Brunak, S. Population-wide
729 analysis of differences in disease progression patterns in men and women. *Nat. Commun.* **10**,
730 666 (2019).

731 56. B, B., J, P. & M, S. Computational solutions for omics data. *Nat. Rev. Genet.* **14**, 333–346
732 (2013).

733 57. Lee, Y. suk *et al.* A Computational Framework for Genome-wide Characterization of the
734 Human Disease Landscape. *Cell Syst.* **8**, 152-162.e6 (2019).

735 58. Robinson, M. D., McCarthy, D. J. & Smyth, G. K. edgeR: A Bioconductor package for
736 differential expression analysis of digital gene expression data. *Bioinformatics* **26**, 139–140
737 (2009).

738 59. Robinson, M. D. & Oshlack, A. A scaling normalization method for differential expression
739 analysis of RNA-seq data. *Genome Biol.* **11**, 184–99 (2010).

740 60. Ritchie, M. E. *et al.* Limma powers differential expression analyses for RNA-sequencing and
741 microarray studies. *Nucleic Acids Res.* **43**, e47 (2015).

61. Johnson, W. E., Li, C. & Rabinovic, A. Adjusting batch effects in microarray expression data using empirical Bayes methods. *Biostatistics* **8**, 118–127 (2007).

62. Van Der Maaten, L. & Hinton, G. Visualizing data using t-SNE. *J. Mach. Learn. Res.* **9**, 2579–2625 (2008).

63. Kanehisa, M. & Goto, S. KEGG: kyoto encyclopedia of genes and genomes. *Nucleic Acids Res.* **28**, 27–30 (2000).

64. Ashburner, M. *et al.* Gene ontology: Tool for the unification of biology. *Nat. Genet.* **25**, 25–29 (2000).

65. Maechler, M. *et al.* Package 'cluster': Cluster Analysis Basics and Extensions. *R topics Documented* 79 (2021).

66. Rousseeuw, P. J. Silhouettes: A graphical aid to the interpretation and validation of cluster analysis. *J. Comput. Appl. Math.* **20**, 53–65 (1987).

67. Chang, W. *et al.* shiny: Web Application Framework for R. *R package* (2021).

68. Pons, P. & Latapy, M. Computing Communities in Large Networks Using Random Walks. *J. Graph Algorithms Appl.* **10**, 191–218 (2006).

69. Clauset, A., Newman, M. E. J. & Moore, C. Finding community structure in very large networks. *Phys. Rev. E - Stat. Physics, Plasmas, Fluids, Relat. Interdiscip. Top.* **70**, 6 (2004).